Available online at www.ijapie.org

INTERNATIONAL JOURNAL OF ADVANCED PRODUCTION AND INDUSTRIAL ENGINEERING

IJAPIE-2017-01-113, Vol 2 (1), 17-22

IJAPIE
Connecting
Science & Technology
with Management.

A Journal for all
Products & Processes.

Eminence of Filler Materials on Metallurgical and Mechanical Properties of GMAW Single Pass SA 240 Grade 304L Weld Joints

Rati Saluja[1], K M Moeed[2]
[1](Mechanical Engineering Department, Goel Institute of Technology & Management, Lucknow, UP, India)
[2](Principal, Integral Polytechnic, Lucknow, UP, India,)
*Email: ratisaluja@gmail.com

Abstract : This analysis is accomplished to characterise significance of ferrite proportion in single pass GMAW on SA 240 Grade AISI 304L austenitic stainless steel welds and its emphasis on microstructural and mechanical properties. These welds were obtained by employing AWS 5.9 AISI 308L, 308LSi and 308 H filler wires. This study intends to divulge the mechanics of austenitic and ferrite microstructure formation and also to institute criterion for its recognition. The investigation was conducted on Grade 304L weld and base material samples using optical and scanning electron microscopy (SEM), microhardness measurements, ferrite measurement and tensile testing. The results revealed that microstructure of fusion zones exhibited a dendrite structure (skeletal and lathy ferrite) weld microstructure and the failure was attributed due to stress corrosion cracking. During tensile strength investigation, weld samples were fractured from heat affected zone.

Keywords: Austenitic Stainless Steel; GMAW; Ferrite; Microhardness; SEM

1. INTRODUCTION

The metallurgy of all stainless steel weld joints is directed by both solidification rate and compositional elements with compositional elements being the major factor. The microstructures of welds in the austenitic steels are austenitic (A), primary austenitic (AF), eutectic (E), primary ferritic (FA), and ferritic (F) [1]. The gradual amplification of the ratio Cr_{eq}/Ni_{eq} results in a shift of the solidification mode from primary austenitic (AF) to primary ferritic (FA) [2]. It may shift within the same fusion zone [3]. Primary ferritic solidification is needed to diminish hot cracking, to provide higher solubility of Sulphur and Phosphorous, thus reducing segregation of these impurities [4]. Existence of ferrite in the austenitic matrix ensures soundness of the joint or its independence from other weld defects [5]. Remedial preheating is not preferable as no structural modifications, such as martensite formation, occur in the weld or HAZ [6].

Therefore, it is essential to identify, role of austenite or ferrite formers as well as promoting elements. [7]. as, compositional elements emphasize stabilization of austenite which plays keyhole in sustaining mechanical properties of the joint. Chromium and Molybdenum acts, first, as active ferrite formers and second as austenite stabilisers. Nickel, Carbon, and Nitrogen also play twin roles, as stable austenite formers as well as, stabilising austenite formation [1,8]. Contribution of Manganese is less in development of austenite but it elevates austenite stability [9].

Quantification of the above influences and their possible results concludes the weld structure, which can be simply predicted by the constitution diagrams for any given weld, The Schaeffler Diagram and WRC 1998 are adopted for determining whether a specified weld metal composition will contain delta ferrite and the approximate percentage. Because of limited toughness and ductility associated with martensite, martensite mixed with ferrite weld structures, extra care is implied in selecting filler materials 300 Series welds [10].

The mechanism of microstructural formation strongly severely affects vulnerability to micro fissuring, hot cracking, the development of delta ferrite, the foundation of sigma phase and stress corrosion cracking [11,20]. Weld metal having a complete austenitic microstructure is significantly more susceptible to formation of above stated situations than weld metal containing low quantity of delta ferrite in an austenitic matrix. Therefore, if practicable, a combination of ferrite matrix in austenitic structure is preferred [12].

Principally, ductility and toughness reduce if the magnitude of ferrite number is above 70, whether for ferrite number less than 30, stress corrosion cracking resistance and strength reduces in austenitic stainless steel [7]. Therefore election of filler metal and welding procedure must be made carefully to secure the small, but necessary magnitude of delta ferrite. According to the WRC, both ASME and NRC have espoused, guidelines of 5FN minimal for the welding consumables to be used in nuclear work to avoid cracking, and 3FN minimal in any multipass weld to restrict fissuring.

Delta ferrite must be confined between FN 4 and FN 21 to evade hot cracking in austenitic stainless steel. Above FN 21, excess delta ferrite results in transformation of

ferrite phase to sigma phase [14].

The magnitude of most filler materials is accustomed by the manufacturers to generate ferrite-containing structures when deposited. The content of Nickel, Chromium, Manganese, Silicon, Copper, Nitrogen, and Niobium restrict the content of delta ferrite, which in turn is balanced by maintaining the ferrite-forming elements on the high side of the allowable ranges, while keeping austenite-forming element low. The quantity of free ferrite in the weld structure will differ with the proportionality of these components.

Therefore to quantify emphasis of ferrite on microstructure, the GMAW process is performed, to predict the suitability of filler materials concerning weld metal by ferrite number (FN), composition and mechanical properties. To recognise the prudish structure and corresponding ferrite numbers (FN) for SA 240 Grade 304L steel prediction tools as well as magnetic induction methods Ferritscope are employed. This article presents a general framework for selection of optimum filler material by predicting delta ferrite for Type 304 L stainless steel welds in gas metal arc welding.

2. EXPERIMENTAL DETAILS

2.1 MATERIALS

48 samples of base material used in the present study were obtained from AISI 304L stainless steel plates with dimensions of (200×100×6) mm with 60^o V-groove. Filler wires as per AWS/ A 5.9 specifications with 2 mm dia have been employed as the GMAW consumables.

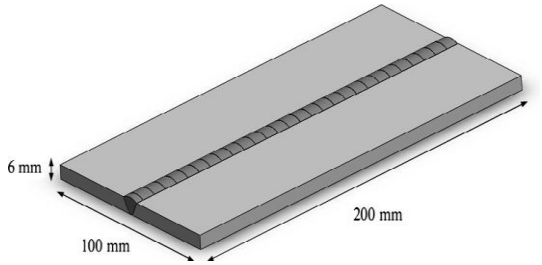

Fig. 1. Schematic illustration of the weldment specimen

2.2. WELDING PROCEDURE

In the welding practice, SA240 Grade AISI 304L steel plates were butt jointed using three filler materials by GMAW process. A single pass bead plate technique is adopted to do GMAW butt welding. Prior to GMAW, all the sample plates were cleaned to uncontaminated mechanically by brushes and chemically by cleaning agents as acetone [15,21].

Table 1 enumerates the chemical compositions of the parent metal and filler wires and welding conditions and parameters are tabulated in Table 2. The lower carbon is present in the previous two filler wires, but silicon, manganese, and interstitials levels are much lower, in vied to other alloys. Filler wires include the elements (Al, Cu, and Ni) essential for secondary hardening.

In the experiments, INMIG-250I welding machine with Direct current electrode positive (DCEP) polarity manufactured by Warp-Engineers Pvt. LTD was used. Commercial Argon + 2 % CO_2 are utilised as the shielding gas in each of the experiments.

Table 1. Chemical composition of parent metal and filler wires, [wt.%]

Type	C	Mn	P	S	Si
304L (plate)	0.03	2.0	0.045	0.03	1.0
308L (filler wire)	0.03	1.0-2.5	0.03	0.03	0.3-0.65
308H (filler wire)	0.04-0.08	1.0-2.5	0.03	0.03	0.3-0.65
308LSi (filler wire)	0.03	1.0-2.5	0.03	0.03	0.65-1.0
Type	Cr	Ni	Mo	N	Cu
304L (plate)	18.0-20.0	8.0-12.0	-	0.10	-
308L (filler wire)	19.5-22.0	9.0-11.0	0.75	0.10	0.75 max
308H (filler wire)	19.5-22.0	9.0-11.0	0.75	0.10	0.75 max
308LSi (filler wire)	19.5-22.0	9.0-11.0	0.75	0.10	0.75 max

Throughout the welding process, joints were visually probed for their quality and it was assured that all weld beads possessed enough geometrical consistency and were free from visible defects like surface porosity, blow-holes etc. Also, argon purge at a rate of 10 lit/min (before welding: 10s and after welding: 4s) was used during welding to prevent penetration of Nitrogen, Oxygen and Hydrogen into the weld pool which could cripple properties of the joint [22]. After welding, specimens were cooled in the air.

Table 2. Manual welding parameters for 304L stainless steel

Current (Amp)	Voltage (Volts)	Gas Flow (lit/min)	Weld speed (inch/min)	Wire feed (inch/min)
85	23	17	19	180

2.3. MACRO AND MICROSTRUCTURAL EXAMINATION

SAMPLE PREPARATION:

Metallographic samples of the cross-section 10x10 mm were incised from welded plates samples followed by coarse and fine grinding on grinding wheels.

The cross-section of the test specimens was mounted and mechanically smoothen to 1200 mesh on Silica Carbide sheets. Subsequently, samples were finally polished on the micro polishing cloth using a suspension of alumina powder and chromium oxide powder on the micro polishing machine.

An aqua-regia reagent HCl: HNO3 (3:1) was used for etching the specimens for the duration of 15 to 20 sec. For weld microstructural identification, scanning electron microscope scrutanised metallographic samples of the joint.

2.3.1 MACRO AND MICROSTRUCTURAL EXAMINATION:

The microstructure of the BM, HAZ and WM was investigated by optical microscopy and scanning electron microscopy (SEM) model- ZEISS EVOMA10 scanning electron microscopy, OLYMPUS SZ-PT stereo microscopy in Research Designs and Standards Organization (RDSO), Lucknow and Delhi Test House, Delhi after preparation by conventional metallographic processes.

INITIAL BASE METAL MICROSTRUCTURE

The micrograph shown in Figure 1(a), is for the Grade 304L base metal which consists an austenitic matrix with equiaxed austenite grains and twins austenitic grains as well [23]. In SEM micrograph of Grade 304L steel, only austenite peaks were observed [17]. Fig. 1(b) displays stereo micrograph of HAZ, WM and BM. The existence of Chromium Carbide leads to intergranular corrosion in austenitic stainless steels.

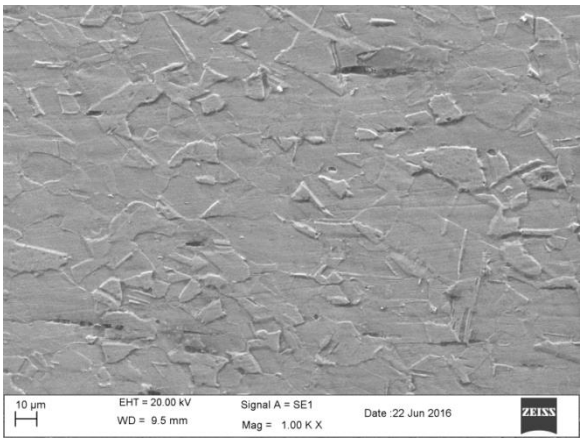

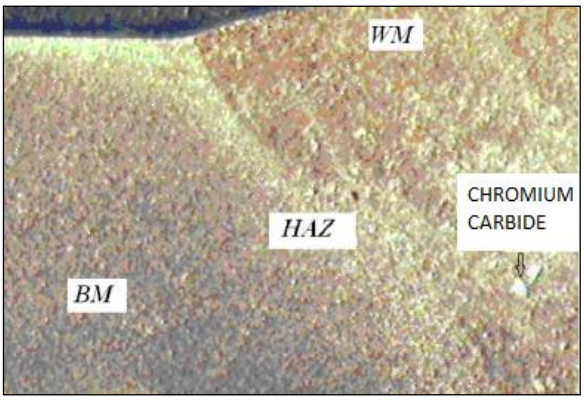

Fig. 1(a): SEM micrographs of base metal (X1000), Fig. 1 (b) Stereo micrographs of HAZ, WM and BM (X200) of 304L

WELD MICROSTRUCTURAL ANALYSIS

Fig. 2 shows SEM image of the dendritic structure present in the welded structure joined by all three filler wires. An epitaxial growth occurred in all specimens as exemplified in Fig. 2 . As it incorporates the grains of weld area to grains of the foundation metal, this type of development is favorable to the welds [22].

Optical Micrography reveals two distinct regions in the microstructure first region belongs to the dendrite phase while another region belongs to the interdendritic phase.

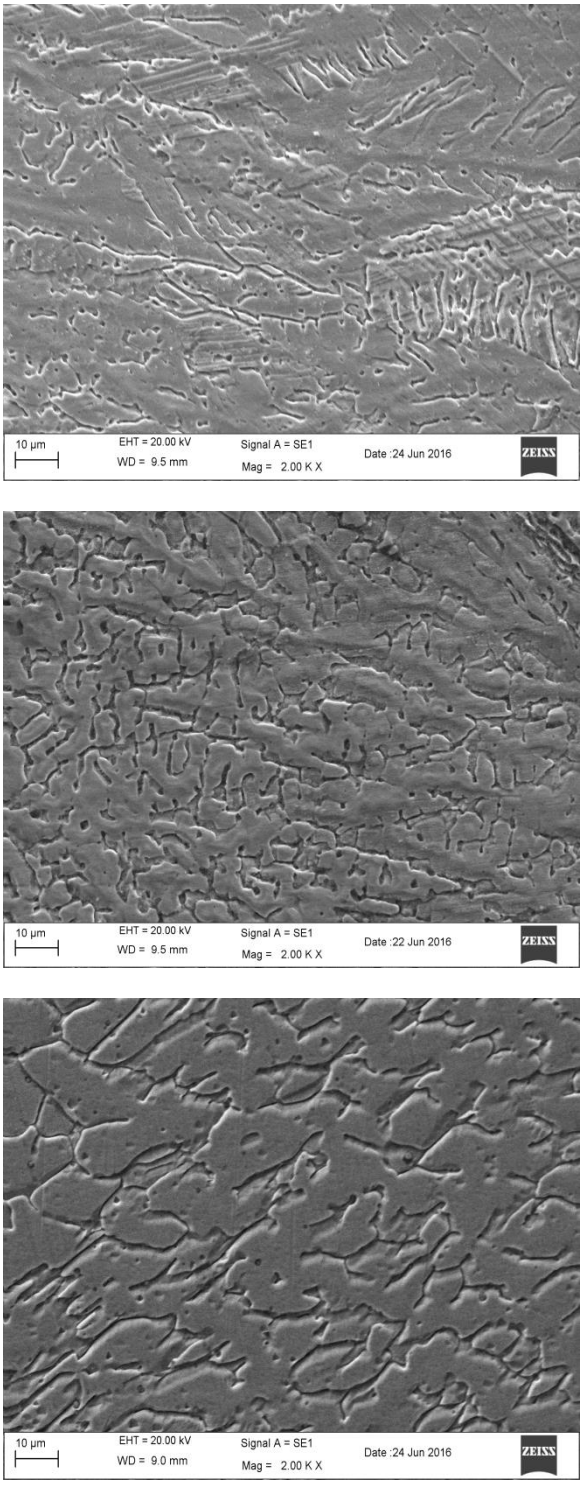

Fig. 2: SEM micrographs of typical dendritic structure accompanied by the interdendritic structure of the weld zone: (a) 308L weld (b) 308LSi (c) 308H (X2000)

It can be concluded that the dendrite phase, is a nickel-enriched phase (austenite) and the interdendritic phase is the chromium enriched phase (δ ferrite). Moreover, according to the SEM image mode, the brighter interdendritic phase has higher chromium content than the dendrite phase [16].

It is clear that two different kinds of lathy δ ferrite and skeletal δ ferrite were formed in the austenite matrix. Similar δ ferrite morphologies were examined in the fusion zone of all weld samples.

Grains were observed to be coarser in the HAZ of AISI 304 in the case of AWS 308H weldments as compared to 308 LSi and 304L weldments. Grains of weldments 308L and 308LSi were found finer than 308H weldment. During the solidification process, the primary δ ferrite solidifies in the fusion zone led by the δ → γ transformation [24].

As a consequence of rapid solidification long dendritic growth at the weld zone in all the weldments take place. As δ→ γ conversion is diffusion controlled process, the rapid cooling rate in GMAW does not tender adequate time to complete this phase transformation. As a result, in weld zone, the primary δ ferrite is retained [13].

While evaluating these micrographs, it is observed that the fusion zones produced by all three filler wires on the Grade 308L steel were free of weld defects like cracking, pores, etc.

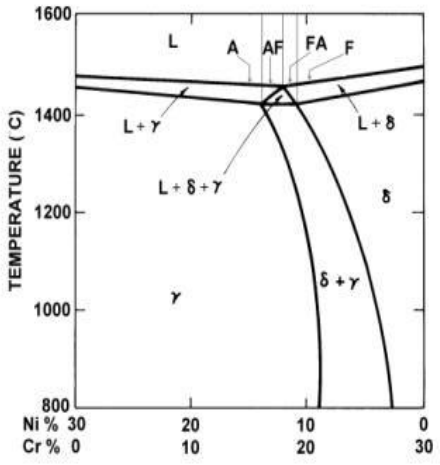

Fig 3. Pseudobinary section of the FE–CR–NI ternary diagram at 70% Fe, showing solidification modes [18]

Liquidus and solidus projections of the Fe–Cr–Ni system (70% Fe) shown along with the constituent binaries is presented in figure 3. It demonstrates that the liquidus projection initiates at the peritectic reaction on the Iron-Nickel system (δ + L↔ γ) and moves down to the eutectic reaction (L↔ γ +δ) on the Chromium- Nickel system in the Fe–Cr–Ni ternary system [18,25]. Most stainless steel compositions in extensive use occur on the iron-rich side of the ternary between 50 and 70 % iron [25].

2.3.2 MICROHARDNESS:

Vickers hardness measurement was carried out by conversion chart (IS:4258) to ascertain the durability. Microhardness measurements were taken in the longitudinal direction. The various areas of interest were identified, like fusion zone (FZ), HAZ as well as the base metal (BM). Despite some instability on the quantified values, a clear trend of continuous variation in hardness of weld zone, base metal, and HAZ is achieved in all No. 1, No. 2 and No. 3 specimens. These behaviours are because of higher amount of δ ferrite in the weld region and coarse grain size in the HAZ. It is widely recognised that the presence of δ ferrite can improve the mechanical strength [15]. Moreover, minimum hardness values were possessed for HAZ of each specimen.

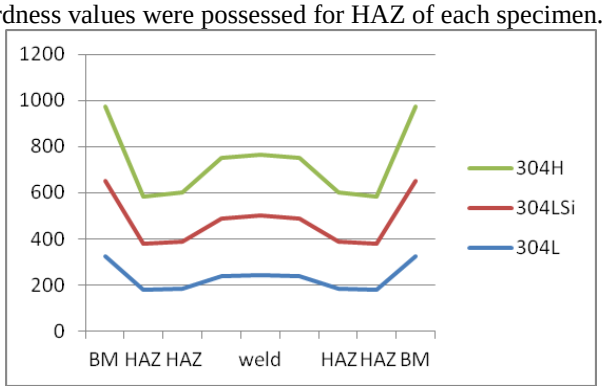

Fig 4. Microhardness profile of different zones of the weldments

The heat evolved from the welding process causes annealing and recovery to take place in the weld zone. It was root leading cause to a drop in hardness [16]. No noticeable change in hardness was revealed for each group of filler wires, although a difference in grain constructions in weld zone is obtained, the highest value of hardness was present in base metal due to more chemical and microstructural homogeneity.

Table3: Hardness range for Weld, HAZ and BM

Grade	Hardness weld	Hardness HAZ	Hardness BM
308L	240-245 HV	180-185 HV	325HV
308LSi	250-255 HV	200-205HV	325HV
308H	260-265 HV	205-210 HV	325HV

The Average hardness value of 262.5HV is examined in 308H weld region of filler material, which is slightly greater than that of the HAZ (207.5 HV) and but lower than parent metal AISI 304. Furthermore, the average hardness value of the weld region of 308LSi (252.5 HV) is slightly higher as compared to HAZ (204.5 HV). Minimum hardness is attained for weld region of 308L (242.5HV) because of low Carbon present. Additionally, it is noticed that the hardness value is higher in weld interface of 308 H (265 HV) GMA weldments.

2.3.3 ULTIMATE TENSILE STRENGTH:

The tensile strengths of all weld joints were assessed. Three specimens were tested and from obtained results average tensile strength was achieved. The tensile test outcomes of the 304 L material joined by GMA welding are given in Table 4. The evaluations were performed in x-direction and with Harriss & Tarriss universal tensile testing machine. The specimens were prepared according to IS:1608.

Table 4. Tensile test results for Grade 304 L austenitic welds

Grade	308L	308LSi	308H	Facture location
UTS (N/MM^2)	473	550	565	HAZ

Tensile test results mainly showed that the fracture occurs away from the joint in each sample plate. Among the three shielded weld metals, ultimate tensile strength of 308LSi and 308H weld metal was higher than the base material (485 N/mm^2). In particular, for 308 H weld, the value of tensile strength is highest, i.e., 565 N/mm^2. The tensile strength of a test plate welded with 308 LSi is found intermediate, and magnitude of ultimate tensile strength was found to be 550 N/mm^2. The tensile strength of weld sample with 308L was found to be 473 N/mm^2.

2.3.4 FERRITE PERCENT

On the basis of the results for Cr_{eq} and Ni_{eq} and using a Schaeffler's diagram can be surmised that delta ferrite is in the interval from 4-16%. The deprivation of Schaeffler Diagram is that it can only account the range of the delta ferrite. Also, in practice for Austenitic steels for which the Schaeffler diagram predicts delta ferrite content of 0-15%, the actual measured content is usually lower than predicted content [6]. WRC 1992 analysis confirmed delta ferrite content ranging from 6.0 to13.0%. It revealed that influence of N_2 on ferrite formation resulted in a reduced value of the nitrogen coefficient in the Nickel equivalent. [11].

Table 5: Delta ferrite content for Grade 304 L austenitic welds

Filler Wire AWS 5.4	Cr_{eq}	Ni_{eq}	Cr_{eq}/ Ni_{eq}	Ferrite %		
				Schaeffler	WRC 1992	Ferritscope
308L	19.35	12.24	1.58	7	6-7	3.23
308H	21.40	12.11	1.76	8-15	8-13	6.22
308 LSi	22.75	13.99	1.63	4-16	6-10	5.87

The magnetic induction technique (MIT) for delta ferrite measurement is preferable for measuring the absolute content of delta ferrite, whereas Schaeffler's Diagram and WRC analysis provide only approximate contents of the ferrite. As displayed in Table 5, comparing between delta ferrite values with other measures, a lower magnitude of delta ferrite by Ferritscope ranging from 0.9 to 7.32 is achieved. Average of all weld samples welded by filler wires 308 L, 308 H and 308LSi has been calculated respectively to obtain final results. The result reveals that delta ferrite for weld produced by AWS 308L is found minimal and maximum for AWS 308H filler wire.

2.4 CONCLUSION

1. Intricate grain structure of microalloyed steels powerfully affects their mechanical properties.
2. A quick cooling cycle with a outsized undercooling will enhance the number of nuclei and thus minimizes the size of resulting dendrites and often lead to small grains leads to higher ductility and vice versa [26].
3. It further reduces hardness and brittleness of the weld.
4. FA and F mode ensure the best resistance to cracking.
5. Higher strength coupled with the high toughness of the weld samples could be equated to the presence of the fine delta-ferrite networks in the weld microstructure [19].
6. Ferrite to austenite formation contributes in increasing the weldment strength.
7. Grains were observed to be coarser in the HAZ of AISI 304 in the case of AWS 308H weldments as compared to 308 LSi and 308L weldments. Long dendritic growth had been witnessed at the weld zone in weldments. Grains of weldments 308L and 308LSi were discerned finer than 308H weldment.
8. Peak hardness values in the weld zone and HAZ were obtained for 308H specimen and then decreased in 308LSi and 308L respectively. Moreover, minimum hardness values were obtained for HAZ of each sample. These behaviors are due to the higher δ ferrite in the weld zone and finer grain size in the HAZ.
9. Tensile test results mainly showed that the fracture occurs away from the joint in each sample plate. Among the three shielded weld metals, ultimate tensile strength of 308LSi and 308H weld metal was higher than the 308L weld metal and base material. Specifically, for 308 H weld, the value of tensile strength is found highest.
10. The weld microstructure consists of grain size 4.5 to 5 in the matrix, whether HAZ comprises Grain size 4.5-4 number. No Inter Granular Corrosion (IGC) observed in welds joined by GMAW.

REFERENCES:

[1] Shankar V. et.al. (2003): Solidification cracking in Austenitic Stainless steel welds, *S¯adhan¯a Vol. 28, Parts 3 & 4* India pp. 359– 382.
[2] Lippold John C. and Kotecki Damian J. (2005): *Welding Metallurgy and Weldability of Stainless Steels*, John Wiley & Sons Inc.
[3] Brooks, J. A., and J. C. Lippold, (1993): Selection of Wrought Austenitic Stainless Steels, *Metals Handbook, Vol. 6*.
[4] Saluja R., Moeed K. M., (2012): The Emphasis of Phase Transformations and Alloying Constituents on Hot Cracking Susceptibility of Type 304L And 316L Stainless Steel Welds, *IJEST, Vol 2, Iss 3*.
[5] Bi◌th M., Monjaret J. L., (2000): Round Robin Test Results on Ultrasonic Testing of Austenitic Welds, *International conference NDE in Relation to Structural Integrity for Nuclear and Pressurized Components, New Orleans*
[6] Suutala, N., Takalo, T., and Moisio, T. (1979). The Relationship between Solidification and Microstructure in Austenitic and Austeniticferritic Stainless Steel Welds. *Metallurgical TransactionsA 10A: 512–514. PP. 2206-2216*
[7] Takalo, T., Suutala, N., and Moisio, T. (1979). Austenitic Solidification Mode in Austenitic

Stainless Steel Welds. *Metallurgical TransactionsA 10A(8): PP.1173–1181.*

[8] Suutala, N., Takalo, T., and Moisio, T.1979. Single Phase Ferritic Solidification Mode in Austenitic-Ferritic Stainless Steel Welds. *Metallurgical Transactions* 10A(8): PP. 1183–1190.

[9] Katayama, S., Fujimoto, T., and Matsunawa, A. (1985). Correlation Among Solidification Process, Microstructure, Microsegregation and Solidification Cracking Susceptibility in Stainless Steel Weld Metals. *Transactions of the JWRI (14)1: PP. 123–138.*

[10] Priceputu I.L., Moisa B., Chiran A., Nicolescu G., Bacinschi Z. (2011): Delta Ferrite Influence in AISI 321 Stainless Steel Welded Tubes, *The Scientific Bulletin of valahia University – Materials and Mechanics , Nr. 6 (year 9)*

[11] R. Saluja and K. M. Moeed, (2015) Formation, Quantification and Significance of Delta Ferrite for 300 Series Stainless Steel Weldments, *International Journal of Engineering Technology, Manage-ment and Applied Sciences*, Vol. 3, PP.23 -36.

[12] https://www.nickelinstitute.org

[13] Lippold, J., and Savage, W. (1980): Solidification of Austenitic Stainless Steel Weldments, Part 2 — The Effect of Alloy Composition on Ferrite Morphology, *Welding Journal* 59(2), PP. 48-s to 58-s.

[14] David, S. (1981): Ferrite Morphology and Variations in Ferrite Content in Austenitic Stainless Steel Welds. *Welding Journal 60(4), PP. 63- 71.*

[15] Rathi V. (2015): Analyzing the Effect of Parameters on SMAW Process, *International Journal of Emerging Research in Management &Technology ISSN: 2278-9359, Volume-4, Issue-6, PP. 16-21.*

[16] Mirshekari G.R., Tavakoli E., Atapour M., Sadeghian B. (2014): Microstructure and Corrosion Behavior of Multipass Gas Tungsten Arc Welded 304L Stainless Steel, *Materials and Design 55, 2014, PP. 905–911.*

[17] Miranda Pérez A. F., Pérez Medina G.Y., Reyes Valdés F.A., Calliari I., Breda M. (2014): Effect of Gas Tungsten Arc Welded 308 and 409 Stainless Steels on their Mechanical Properties, *La Metallurgia Italiana, PP. 49-53.*

[18] Iamboliev T., Katayama S., and Matsunawa A. (2003): Interpretation of Phase Formation in Austenitic Stainless Steel Welds**,** Criteria for Mechanism Identification of Fully Austenitic Weld Metal formation are recommended, *WRC, pp.337-347.*

[19] Samantaray D., Kumar V., Bhaduri K., Dutta P. (2012), Microstructural Evolution and Mechanical Properties of Type 304 L Stainless Steel Processed in Semi-Solid State, *International Journal of Metallurgical Engineering.*

[20] Shiri, Sajjad Gholami, Mohsen N., Mahmood S.,et. al.(2012): "Gas tungsten arc welding of CP-copper to 304 stainless steel using different filler materials", *Transactions of Nonferrous Metals Society of China*.

[21] Kumar, S.:(2011) "Effect of heat input on the microstructure and mechanical properties of gas tungsten arc welded AISI 304 stainless steel joints", *Materials and Design.*

[22] Shoja Razavi, Reza.:(2016) "Laser beam welding of Waspaloy: Characterization and corrosion behavior evaluation", *Optics & Laser Technology.*

[23] https:// aimnet.it

[24] Lu, B.T.:(2005). "Pitting and stress corrosion cracking behavior in welded austenitic stainless steel", *Electrochimica Acta*

[25] https:// www.ias.ac.in

[26] https://steelguru.com